

Magnetic properties of DyCrO₃

A. M. Kadomtseva, A. K. Zvezdin, A. A. Mukhin, I. A. Zorin, I. B. Krynetskii, M. D. Kuz'min, and M. M. Lukina

Moscow State University

(Submitted 12 May 1986)

Zh. Eksp. Teor. Fiz. **92**, 179–189 (January 1987)

The magnetic properties of DyCrO₃ and the phase transitions in it are investigated in the range $T = 1.6\text{--}150$ K in magnetic fields up to 60 kOe. It is shown that Dy³⁺ behaves as an Ising ion with an essay axis located in the ab plane at an angle $\pm 63^\circ$ to the a axis. The effective field ($H_{\text{eff}}^x = 3.5$ kOe) that causes splitting of the ground doublet of the Dy³⁺ ion in the Γ_2 phase is determined. The orientational transition $\Gamma_{42} \rightarrow \Gamma_2$ induced by a field $\mathbf{H} \parallel \mathbf{c}$ is investigated and the H_z - T phase diagram is plotted. The mechanisms responsible for the high anisotropy energy in the ac plane are discussed. The metamagnetic transitions observed in DyCrO₃ are consistently analyzed with account taken of the renormalization of the Dy–Dy interaction constants by isotropic Dy–Cr exchange.

Rare-earth orthochromites (RCrO₃) are compounds having the same structure as orthoferrites (RFeO₃); their crystal symmetry is described by the rhombic space group $D_{2h}^{16} \cdot Pbnm$.^{1/2} Despite a number of magnetic properties shared by orthoferrites and orthochromites, substantial differences are observed in their magnetic anisotropy, in the character of the spin-reorientation transitions, and in other properties. Dysprosium orthochromite and orthoferrite differ particularly strongly in their magnetic behavior. It is known that as the temperature is lowered to 40 K a spin-reorientation transition is observed in DyFeO₃, from a weakly ferromagnetic state to an antiferromagnetic state ($G_x F_z - G_y$), which is preserved also after the Dy³⁺-ion spins are ordered at $T_{N2} = 3.7$ K.^{3,5} In contrast to dysprosium orthoferrite, DyCrO₃ has a magnetic structure $G_z F_x$ (Γ_2); for the spins of the Cr³⁺ ions at all temperatures below $T_{N1} = 142$ K; at $T_{N2} \approx 2$ K the spins of Dy³⁺ become ordered in accord with the Γ_{25} ($f_x c_y g_x a_y$) mode, without disturbing the magnetic structure of the chromium sublattice.^{6,7} At low temperatures ($T < T_{N2}$) metamagnetic transitions are observed both in DyCrO₃ (Refs. 7 and 8) and in DyFeO₃ (Ref. 3). The character of these transitions, however differs qualitatively when \mathbf{H} is parallel to the a axis. We deemed it of interest to investigate in greater detail the magnetic properties of dysprosium orthochromite (in a wider range of temperatures and of magnetic fields), with an aim to elucidating the features of the anisotropic Dy–Cr interaction that is responsible for the special magnetic behavior of DyCrO₃.

EXPERIMENTAL RESULTS AND DISCUSSION

1. Experiment

Single crystals of DyCrO₃ were grown from the molten solution using isothermal evaporation. The magnetization curves at various orientations of the magnetic field were measured with a vibration magnetometer in a superconducting-solenoid field up to 60 kOe at temperatures from 1.6 to 140 K.

Figure 1 shows the low-temperature magnetization curves of DyCrO₃ along the a , b , and c axes of a rhombic crystal (the x , y , and z axes, respectively). It can be seen that the magnetization is strongly anisotropic and is a maximum

along the crystal b axis. In strong field, the magnetization along the a and b axes saturates at 88 and 175 G·cm³/g, respectively. The magnetization along the c axis is a minimum and varies practically linearly with increase of the field, the specific susceptibility being $\chi_z = 1.8 \cdot 10^{-4}$ cm³/g. The magnetization curves were most complicated along the a axis of the crystal at temperatures below $T_{N2} = 2$ K, where the Dy³⁺-ion spins are ordered in accord with the $g_x a_y$ (Γ_5) mode. In the low temperature region ($T < T_{N2}$) for $\mathbf{H} \parallel \mathbf{a}$, just as in Ref. 7, two jumps were observed on the magnetization curve and corresponded to two metamagnetic $g_x a_y \rightarrow f_y f_x \rightarrow c_y f_x$ transitions in the Dy subsystem.

The spontaneous magnetization m_x of the crystal in the phase Γ_2 increased almost parabolically with decrease of temperature, reaching at liquid-helium temperature a smeared-out maximum of 13 G·cm³/g, and then decreased steeply below T_{N2} to a value $m_x = 5.5$ G·cm³/g (Fig. 2). The susceptibility along the a and b axes of the crystal followed the Curie-Weiss law at high temperature (Fig. 3), while a gently sloping maximum was observed in the $\chi_y(T)$ and $\chi_x(T)$ plots in the Dy³⁺-ion ordering region.

Measurements of the magnetization curves along the c axis of the crystal, carried out in the temperature range 1.9–140 K, have shown that the specific susceptibility χ_z is low ($\approx 2 \cdot 10^{-4}$ cm³/g) and varies little with temperature below 100 K (Fig. 4). At temperatures higher than 65 K the magnetization curves, for a sufficiently high threshold magnetic field H_z^{th} , show kinks corresponding to the spin reorienta-

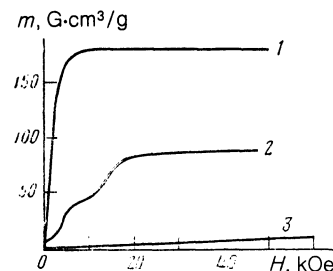


FIG. 1. Magnetization curves of single-crystal DyCrO₃: 1— $\mathbf{H} \parallel \mathbf{b}$ ($T = 1.65$ K); 2— $\mathbf{H} \parallel \mathbf{a}$ ($T = 1.61$ K); 3— $\mathbf{H} \parallel \mathbf{c}$ ($T = 4.2$ K).

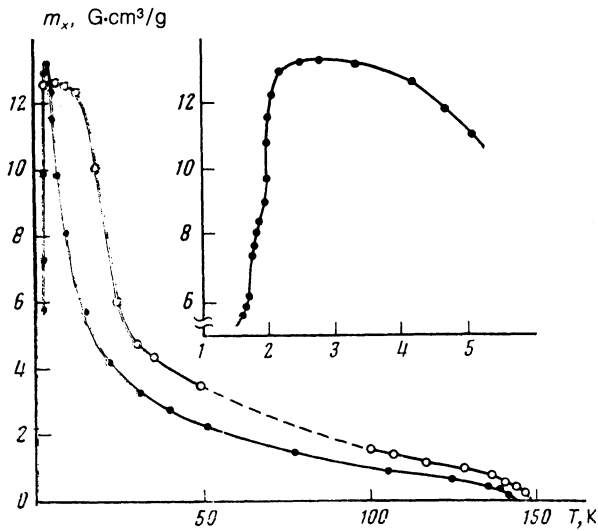


FIG. 2. Temperature dependence of the spontaneous magnetization along the a axis of DyCrO_3 : ●—our measurement data, ○—data of Ref. 7.

tion $G_{zx}F_{xz} - G_xF_z$ (inset in Fig. 5). The threshold field decreased with increase of temperature and vanished at the Néel point (Fig. 5). In this temperature region the initial susceptibility was increased (Fig. 4) by the additional susceptibility due to rotation of the Cr^{3+} -ion spins. At low T , the fields ≈ 60 kOe at our disposal were not strong enough to cause the spin-reorientation transition $G_{zx}F_{xz} - G_xF_z$, attesting to the strong increase of the anisotropy in the ac plane.

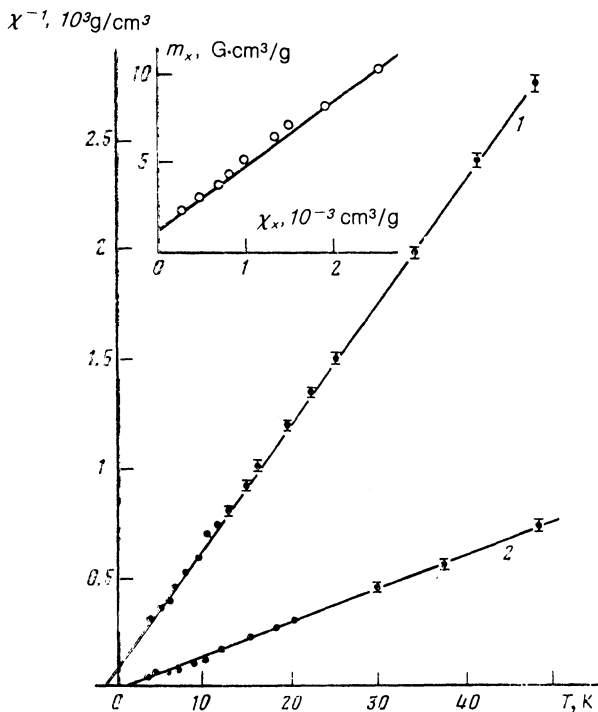


FIG. 3. Temperature dependence of the reciprocal susceptibility: 1—along the a axis, 2—along the b axis. Inset— $m_x(\chi_x)$ dependence.

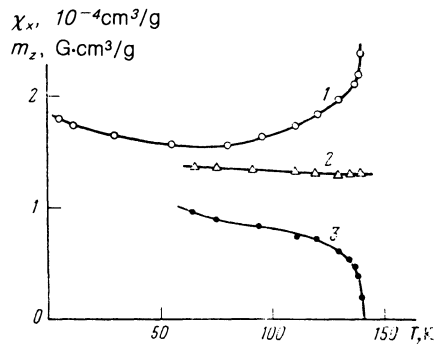


FIG. 4. Temperature dependences of the susceptibility along the c axis (1— χ_z in phase Γ_2 at $H=0$; 2— χ_z in phase Γ_4) and of the induced magnetization along the c axis (3).

2. Spin Hamiltonian of Dy^{3+} ions and thermodynamic potential of DyCrO_3

To describe the observed magnetic properties of DyCrO_3 at $T \lesssim 50$ K we need only the Dy^{3+} -ion ground doublet, which is separated from the excited states by ≈ 50 cm^{-1} [according to the optical data for Dy^{3+} in DyFeO_3 (Ref. 9) and DyAlO_3 (Ref. 10)]. According to our experimental results, the behavior of the Dy^{3+} ion at low temperatures is strongly anisotropic (see Fig. 1) and is close in fact to an Ising ion with an anisotropy axis in the ab plane. It follows from the saturation magnetizations along the a and b axes that the Ising axis of the Dy^{3+} ions makes an angle $\pm \alpha = \pm 63^\circ$ with the a axis, and the magnetic moment along this axis is $\mu_0 = 9.1 \mu_B$. Similar Ising behavior of the Dy^{3+} ion with like values of α and μ_0 is observed in DyFeO_3 (Ref. 3) and DyAlO_3 (Ref. 11).

The spin Hamiltonian of Dy^{3+} ions can be represented in the Ising approximation for four rare-earth sublattices in the form

$$\mathcal{H}_{\text{eff}}^i = -\mu_0 \sigma_{zi} \mathbf{n}_i \cdot (\mathbf{H} + a_0 \mathbf{F} + \hat{P}_i \mathbf{G} + \mathbf{H}_i^R) + \Delta E_{vv}^i(\mathbf{H}, \mathbf{F}, \mathbf{G}), \quad (1)$$

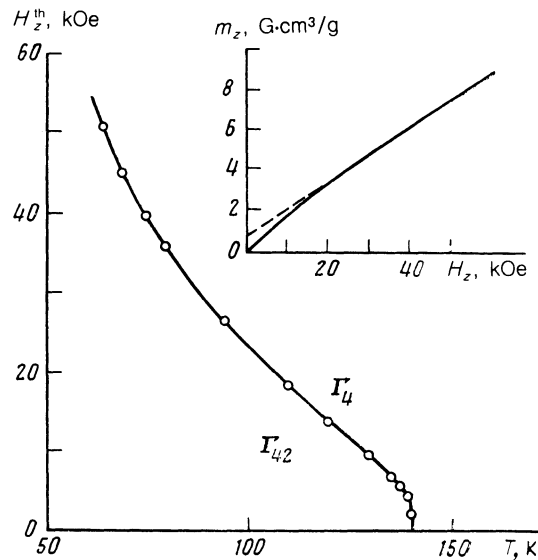


FIG. 5. H_2 - T phase diagram for DyCrO_3 . The inset shows a typical magnetization curve $m(H)$ in the temperature region where the $\Gamma_{4,2} \rightarrow \Gamma_2$ spin-reorientation transition was induced ($T = 111$ K).

where σ_{zi} is the z component of the Pauli matrix of the Dy^{3+} ions for the i th sublattice ($i = 1, 2, 3, 4$); \mathbf{F} and \mathbf{G} are the dimensionless ferro- and antiferromagnetism vectors of the Cr subsystem; \mathbf{H} is the external magnetic field; \mathbf{H}_i^R is the effective field applied to the i th Dy^{3+} ion by the other Dy^{3+} ions; $\mathbf{n}_i = (\cos \alpha, \pm \sin \alpha, 0)$ is a unit vector along the Ising axis; a_0 is the constant of the Dy–Cr isotropic interaction; and

$$\hat{P}_i = \begin{pmatrix} 0 & 0 & p_{xz} \\ 0 & 0 & \pm p_{yz} \\ p_{zx} & \pm p_{zy} & 0 \end{pmatrix}$$

is the matrix of the anisotropic Dy–Cr interaction.⁵ The \pm signs in \mathbf{n}_i and \hat{P}_i refer respectively to positions (Dy^{3+} sublattices) 1, 2, and 3, 4.

The quantities ΔE_{VV}^i (\mathbf{H} , \mathbf{F} , \mathbf{G}) in (1) take into account the shift of the centroid of the Dy^{3+} -ion doublet through mixture of excited state via the Dy–Cr exchange interaction and via the interaction with the external field. These quantities are equivalent to the familiar contributions to the magnet energy from the Van Vleck paramagnetism. We do not specify the explicit form of ΔE_{VV} , but will take it into account below by renormalizing the coefficients of the Cr-subsystem thermodynamic potential.

We shall analyze the DyCrO_3 magnetic properties and phase transitions on the basis of the nonequilibrium-state thermodynamic potential which can be represented, according to Ref. 12 and with allowance for Eq. (1), in the form

$$\Phi(\mathbf{F}, \mathbf{G}, \sigma_i) = \Phi_{\text{Cr}}(\mathbf{F}, \mathbf{G}) - N[f\mu_0 \cos \alpha (H_x + a_0 F_x + p_{xz}' G_z) + c\mu_0 \sin \alpha (H_y + a_0 F_y)] + \langle \mathcal{H}_{\text{R-R}} \rangle - \frac{1}{4} N T \sum_{i=1}^4 S(\sigma_i), \quad (2)$$

where $\sigma_i = \langle \sigma_{zi} \rangle$ is the mean value of the Pauli matrix of the i th Dy^{3+} ion and constitutes its relative magnetic moment along the Ising axis;

$$f = (\sigma_1 + \sigma_2 + \sigma_3 + \sigma_4)/4, \quad c = (\sigma_1 + \sigma_2 - \sigma_3 - \sigma_4)/4, \\ g = (\sigma_1 - \sigma_2 + \sigma_3 - \sigma_4)/4, \quad a = (\sigma_1 - \sigma_2 - \sigma_3 + \sigma_4)/4$$

are quantities that define the basis vectors of the R subsystem¹⁾;

$$\Phi_{\text{Cr}}(\mathbf{F}, \mathbf{G}) = \frac{1}{2} A \mathbf{F}^2 + \frac{1}{2} \sum_k b_k G_k^2 - d(F_x G_z - F_z G_x) - M_0 \mathbf{F} \mathbf{H} - \frac{1}{2} \sum_k \chi_k^{\text{VV}} H_k^2 - \tau_1^{\text{VV}} H_x G_z - \tau_3^{\text{VV}} H_z G_x \quad (k = x, y, z) \quad (3)$$

is the Cr-subsystem thermodynamic potential renormalized by the Van Vleck contribution ΔE_{VV} to (1), $b_k = b_k^{\text{VV}}$. For the temperatures considered ($T \lesssim 50$ K), all the coefficients in (3) depend little on T , while \mathbf{F} and \mathbf{G} are connected by the relations $\mathbf{F}^2 + \mathbf{G}^2 = 1$ and $\mathbf{F} \cdot \mathbf{G} = 0$;

$$S(\sigma) = \ln 2 - \frac{1}{2} (1 + \sigma) \ln(1 + \sigma) - \frac{1}{2} (1 - \sigma) \ln(1 - \sigma)$$

is the entropy of the two-level system; N is the number of rare-earth ions per gram;

$$\langle \mathcal{H}_{\text{R-R}} \rangle = -\frac{1}{8} N \sum_{i,j=1}^4 \sigma_i T_{ij} \sigma_j = -\frac{1}{2} N (\Theta_2 f^2 + \Theta_3 c^2 + \Theta_5 g^2 + \Theta_6 a^2), \quad (4)$$

is the energy of the R–R interaction, in which the subscripts of the constants Θ_α of the R–R interactions are equal to the numbers of the irreducible representation (Γ_1 to Γ_8) according to which the R subsystem is ordered (polarized); $p'_{xz} = p_{xz} + p_{y2} \tan \alpha$.

3. High-temperature properties; susceptibility, magnetization, H_z - T phase diagram

At relatively high temperatures ($T > T_{N2}$) and in a weak magnetic field ($\mu_0 H \ll k_B T$) the Dy-system magnetic moments are not saturated, i.e., $\sigma_i \ll 1$. Expanding $S(\sigma_i)$ up to quadratic terms and minimizing (2) with respect to f and c (since $g = a = 0$ for $T > T_{N2}$), we express them in terms of \mathbf{F} , \mathbf{G} , and \mathbf{H} and represent the thermodynamic potential in the form

$$\Phi(\mathbf{F}, \mathbf{G}) = \frac{1}{2} \sum_k (A_k F_k^2 + \tilde{b}_k G_k^2) - d_1 F_x G_z - d_3 F_z G_x - M_0 \sum_k (1 + \eta_k) F_k H_k - (\tau_1 + \tau_1^{\text{VV}}) H_x G_z - \tau_3^{\text{VV}} H_z G_x - \frac{1}{2} \sum_k (\chi_k^{\text{R}} + \chi_k^{\text{VV}}) H_k^2 \quad (k = x, y, z), \quad (5)$$

where

$$\chi_x^{\text{R}} = N\mu_0^2 \cos^2 \alpha / (T - \Theta_2), \quad \chi_y^{\text{R}} = N\mu_0^2 \sin^2 \alpha / (T - \Theta_3), \\ \chi_z^{\text{R}} = 0, \quad A_k = A - \chi_k^{\text{R}} a_0^2, \quad \eta_k = a_0 \chi_k^{\text{R}} / M_0, \quad \tilde{b}_{x,y} = b_{x,y}, \\ \tilde{b}_z = b_z - \chi_x^{\text{R}} (p_{xz}')^2, \quad \tau_1 = \chi_x^{\text{R}} p_{xz}', \quad d_1 = d + a_0 \tau_1, \quad d_3 = -d. \quad (6)$$

In the Γ_2 ($G_z F_x$) phase that is realized in DyCrO_3 at $T > T_{N2}$, the spontaneous magnetic moment m_x and the initial magnetic susceptibilities χ_x and χ_y are expressed in terms of the parameters of the thermodynamic potential (5) as follows:

$$\chi_x = \chi_1^{\text{Cr}} + \chi_x^{\text{VV}} + N\mu_0^2 \cos^2 \alpha / (T - \tilde{\Theta}_2), \\ \chi_y = \chi_1^{\text{Cr}} + \chi_y^{\text{VV}} + N\mu_0^2 \sin^2 \alpha / (T - \tilde{\Theta}_3), \\ m_x = m_{x0} + [N\mu_0^2 \cos^2 \alpha / (T - \tilde{\Theta}_2)] H_{\text{eff}}^x, \quad (7)$$

where

$$\chi_{\perp}^{\text{Cr}} = M_0^2 / A \equiv M_0 / 2H_E, \quad m_{x0} = (M_0 d / A + \tau_1^{\text{VV}}) G_{z0}, \\ H_{\text{eff}}^x = (p_{xz}' + a_0 d / A) G_{z0}, \quad G_{z0} = \pm 1, \\ \tilde{\Theta}_2 = \Theta_2 + N(\mu_0 a_0 \cos \alpha)^2 / A, \quad \tilde{\Theta}_3 = \Theta_3 + N(\mu_0 a_0 \sin \alpha)^2 / A,$$

$\tilde{\Theta}_2$ and $\tilde{\Theta}_3$ are the Dy-subsystem paramagnetic Curie temperatures renormalized by the Dy–Cr isotropic exchange interaction.

The observed temperature dependences of the susceptibilities χ_x and χ_y and of the magnetization m_x in the temperature interval 5–50 K are described by Eqs. (7) with the following parameters:

$$\mu_0 = (8 \pm 1) \mu_B, \quad \alpha = 63 \pm 2^\circ, \quad \Theta_2 = (-2 \pm 0.5) \text{ K}, \\ \tilde{\Theta}_3 = (1 \pm 1) \text{ K}, \quad H_{\text{eff}}^x = (3.5 \pm 0.3) \text{ kOe}, \\ m_{x0} = (1.3 \pm 0.2) \text{ G} \cdot \text{cm}^3 / \text{g}.$$

The quantities χ_1^{Cr} and $\chi_{x,y}^{\text{VV}}$ can be neglected in this temperature interval. The inset of Fig. 3 illustrates the linear

dependence of the magnetization m_x on the susceptibility χ_x from which H_{eff}^x was determined. The obtained values of μ_0 and α agree with the corresponding parameters obtained above from the saturation magnetizations along the a and b axes.

We discuss now the behavior of DyCrO₃ in a field $\mathbf{H}||c$, which causes rotation of the Cr-subsystem spins in the ac plane and which leads to a transition to the configuration Γ_4 ($G_x F_z$) when the threshold field $H_z^{\text{th}}(T)$ is reached. The threshold field is determined by the expression

$$\begin{aligned} H_z^{\text{th}} &= -|m_z - 2m_z'|/2\chi_{\perp}^{\text{Cr}} + \{ [(m_z - 2m_z')/2\chi_{\perp}^{\text{Cr}}]^2 + K_{ca}/\chi_{\perp}^{\text{Cr}} \}^{1/2}, \\ m_z &= (-M_0 d/A + \tau_3^{\text{VV}})G_{x0}, \\ m_z' &= -(M_0 a_0/A)\chi_x^{\text{R}}(p_{xz}' + a_0 d/A)G_{x0}, \\ G_{x0} &= \pm 1, \quad K_{ca} = b_x - b_z + \chi_x^{\text{R}}(H_{\text{eff}}^x)^2, \end{aligned} \quad (8)$$

where m_z is the spontaneous weak ferromagnetic moment in the Γ_4 ($G_x F_z$) phase, and K_{ca} is the effective anisotropy constant in the ac plane.

The magnetization curves, whose kinks were used to determine $H_z^{\text{th}}(T)$, consist each of two linear segments (inset of Fig. 5):

$$\begin{aligned} m_z(H_z) &= m_z + \chi_z H_z, \quad H_z > H_z^{\text{th}}, \\ m_z(H_z) &= \chi_z^0 H_z, \quad H_z < H_z^{\text{th}}, \end{aligned} \quad (9)$$

where $\chi_z = \chi_z^{\text{Cr}} + \chi_z^{\text{VV}}$ is the susceptibility in the Γ_4 phase, while $\chi_z^0 = \chi_z^{\text{VV}} + \chi_z^{\text{rot}}$ is the initial susceptibility in the Γ_2 phase, and $\chi_z^{\text{rot}} \approx (m_z + m_z')^2/K_{ca}$ is the rotational susceptibility. Comparison of the experimental temperature dependences of the susceptibilities χ_z and χ_z^0 with the theoretical ones shows that the main contribution to χ_z is made by the Van Vleck susceptibility χ_z^{VV} of the Dy³⁺ ions. The quantity χ_1^{Cr} in χ_z can be neglected compared with χ_z^{VV} , since $\chi_1^{\text{Cr}} \approx 1.4 \cdot 10^{-5}$ cm³/g (Ref. 13). The difference between the initial susceptibility χ_z^0 and χ_z for $T > 50$ K is due to the contribution made to χ_z^0 by the rotational susceptibility which increases with temperature because the anisotropy energy in the ac plane is decreased. This is attested also by the decrease of $H_z^{\text{th}}(T)$ with increase of T . Putting

$$\begin{aligned} \chi_{\perp}^{\text{Cr}} &= 1.4 \cdot 10^{-5} \text{ cm}^3/\text{g}, \quad m_z \approx 1 \text{ G} \cdot \text{cm}^3/\text{g}, \\ |m_z'| &\ll m_z, \quad H_z^{\text{th}}(60\text{K}) = 55 \text{ kOe}, \end{aligned}$$

we obtain from (8)

$$K_{ca}(60 \text{ K}) \approx 9.7 \cdot 10^4 \text{ erg/g.}$$

Note that so high an anisotropy energy cannot be provided by the Zeeman contribution $\chi_x^{\text{R}}(H_{\text{eff}}^x)^2$ to K_{ca} , a contribution connected with the anisotropy of the splitting of the ground doublet of the Dy³⁺ ion. At 60 K this contribution is only $0.38 \cdot 10^4$ erg/g. Taking this circumstance into account, and also the fact that the Cr-subsystem contribution $K_{ca}^{\text{Cr}} = b_x^{\text{Cr}} - b_z^{\text{Cr}}$ is apparently negative and stabilizes the Γ_4 configuration (as in YCrO₃), we conclude that in the ac plane the Van Vleck contribution $K_{ca}^{\text{VV}} = b_x^{\text{VV}} - b_z^{\text{VV}}$ to the anisotropy energy is large. Another possible mechanism that gives rise to a large value of K at high temperatures is the anisotropy of the Zeeman splitting of the excited Dy³⁺-ion doublets.

Comparison of the behavior of the Dy³⁺ ions in

DyCrO₃ and DyFeO₃ and of their interaction with the d -subsystem points to definite differences. Thus, the Van Vleck contribution χ_z^{VV} to the susceptibility along the c axis is almost twice as small in DyCrO₃ as in DyFeO₃. The Van Vleck contribution to the anisotropy in the ac plane of DyCrO₃ is very large compared with DyFeO₃. All this may be due to the difference between the wave functions of the excited Dy³⁺-ion doublets in the crystal fields of these compounds, and also to the difference between the values of the Dy–Cr and Dy–Fe anisotropic exchange parameters.

4. Low-temperature properties; metamagnetic transitions

To describe the observed behavior of DyCrO₃ in the region where the Dy³⁺ ions are antiferromagnetically ordered, we begin with the thermodynamic potential (2). Minimizing it with respect to \mathbf{F} and recognizing that $\mathbf{F} \cdot \mathbf{G} = 0$ and $\mathbf{G}^2 = 1 - \mathbf{F}^2 \approx 1$, we represent the potential at $\mathbf{H}||c$ in the form

$$\begin{aligned} \Phi(\sigma_i) &= \Phi_0 + \langle \tilde{\mathcal{H}}_{\text{R-R}} \rangle - 1/4 N \left[h_x(\sigma_1 + \sigma_2 + \sigma_3 + \sigma_4) \right. \\ &\quad \left. + h_y(\sigma_1 + \sigma_2 - \sigma_3 - \sigma_4) + T \sum_{i=1}^4 S(\sigma_i) \right] \end{aligned} \quad (10)$$

where

$$\begin{aligned} h_x &= \mu_0(H_x + H_{\text{eff}}^x) \cos \alpha, \quad h_y = \mu_0 H_y \sin \alpha, \\ \langle \tilde{\mathcal{H}}_{\text{R-R}} \rangle &= -1/4 N [1/2 \tilde{T}_{11}(\sigma_1^2 + \sigma_2^2 + \sigma_3^2 + \sigma_4^2) \\ &\quad + \tilde{T}_{12}(\sigma_1 \sigma_2 + \sigma_3 \sigma_4) + \tilde{T}_{13}(\sigma_1 \sigma_3 + \sigma_2 \sigma_4) + \tilde{T}_{14}(\sigma_1 \sigma_4 + \sigma_2 \sigma_3)], \end{aligned} \quad (11)$$

\tilde{T}_{ij} are the Dy–Dy interaction constant renormalized by the Dy–Cr interactions; they are connected with $\tilde{\Theta}_2, \tilde{\Theta}_3, \Theta_5, \Theta_8$ by the relations

$$\begin{aligned} \tilde{T}_{14} &= (\tilde{\Theta}_2 + \tilde{\Theta}_3 + \Theta_5 + \Theta_8)/4, \quad \tilde{T}_{12} = (\tilde{\Theta}_2 + \tilde{\Theta}_3 - \Theta_5 - \Theta_8)/4, \\ \tilde{T}_{13} &= (\Theta_2 - \Theta_3 + \Theta_5 - \Theta_8)/4, \quad \tilde{T}_{14} = (\Theta_2 - \Theta_3 - \Theta_5 + \Theta_8)/4, \end{aligned} \quad (12)$$

$\tilde{\Theta}_2$ and $\tilde{\Theta}_3$ are defined in (7). We have put $|G_z| = 1$ in (10), since the field satisfies $\mathbf{H}||c$ and does not change the orientation of \mathbf{G} .

Let us use (10) to analyze the metamagnetic transitions observed in DyCrO₃. Of greatest interest here is the cause of the two-step metamagnetic transition at $\mathbf{H}||a$ and of the role played here by the d -subsystem, since in DyAlO₃ and DyFeO₃ the metamagnetic transitions usually observed are one-step. Note that metamagnetic transitions in DyCrO₃ were analyzed in Ref. 8, where it was shown that for certain relations between the Dy–Dy interaction constants the metamagnetic transition at $\mathbf{H}||a$ can be two-step, and that an important role is played by the Cr subsystem that mediates an additional indirect Dy–Dy exchange interaction of the Suhl–Nakamura type¹⁴ (see also Ref. 15). In the thermodynamic potential obtained above this interaction is taken into account automatically by renormalization of the R–R interaction constants. This permits a more consistent analysis of the influence of the d -subsystem on the metamagnetic transitions.

Let us consider the case $T = 0$. The equilibrium directions of σ_i are determined from the equations

$$\sigma_i = \text{sign}(h_x \pm h_y + h_i^{\text{R}}), \quad (13)$$

where $h_i^R = -(4/N)\partial(\mathcal{H}_{R-R})/\partial\sigma_i$, and the \pm signs pertain respectively to $i = 1, 2$ and $3, 4$. As a result, the following phases are possible in the system:

a) antiferromagnetic phase $A(a_y g_x)$, in which

$$\sigma_1 = \sigma_3 = -\sigma_2 = -\sigma_4 = \pm 1;$$

b) antiferromagnetic phase $A'(a_x g_y)$, in which

$$\sigma_1 = \sigma_4 = -\sigma_2 = -\sigma_3 = \pm 1$$

(since the Dy^{3+} ions are ordered in DyCrO_3 in accordance with the representation $\Gamma_5(a_y g_x)$, the phase A is favored over A' , leading to the constraint $T_{14} < T_{13}$ on the constants);

c) ferromagnetic phase $B(f_x c_y)$ with $\sigma_i = 1$;

d) ferromagnetic phase $C(f_y c_x)$ in which

$$\sigma_1 = \sigma_2 = -\sigma_3 = -\sigma_4 = 1;$$

d) intermediate phase $D(f_{xy} c_{xy} a_{xy} g_{xy})$, in which

$$\sigma_1 = \sigma_2 = 1, \quad \sigma_3 = -\sigma_4 = \pm 1.$$

Phases A and D , D and B , and D and C have stability regions that overlap if the condition $T_{11} > 0$ is met. For the phase pairs A and B and A and C the corresponding conditions are $T_{11} + T_{12} > 0$ and $T_{12} - T_{14} > 0$, respectively. The metamagnetic-transition lines on the $h_x - h_y$ plane can be obtained by equating the energies of the corresponding phases:

$$\begin{aligned} A \leftrightarrow D: h_x + h_y &= -\tilde{T}_{12} + \tilde{T}_{13} - \tilde{T}_{14}, \\ D \leftrightarrow B: h_x - h_y &= -\tilde{T}_{12} - \tilde{T}_{13} - \tilde{T}_{14}, \\ D \leftrightarrow C: h_x - h_y &= \tilde{T}_{12} - \tilde{T}_{13} - \tilde{T}_{14}, \\ A \leftrightarrow B: h_x &= -\tilde{T}_{12} - \tilde{T}_{14}, \\ A \leftrightarrow C: h_y &= -\tilde{T}_{12} + \tilde{T}_{13}. \end{aligned} \quad (14)$$

In the general case, if $h_x \neq 0$ and $h_y = 0$, the two-step metamagnetic transitions $A \rightarrow D \rightarrow B$ or $A \rightarrow D \rightarrow C$ are possible in the system (Fig. 6).

Let us ascertain the conditions under which the two-step metamagnetic transition $A \rightarrow D \rightarrow B$ is possible in a field directed strictly along the a axis. Obviously, this calls for the field $h_{x0} = -\tilde{T}_{12} - \tilde{T}_{14}$ of the $A \rightarrow B$ transition to be stronger than the field $h_{x1} = h_{x0} + \tilde{T}_{13}$ of the $A \rightarrow D$ transition, so that the following inequality holds:

$$T_{13} = T_{13} + 1/4(\mu_0^2 a_0^2 / 2H_E \mu_{Cr}) \cos 2\alpha < 0. \quad (15)$$

Since $\cos 2\alpha < 0$ and the constant T_{13} that determines the

interaction of widely separated ions in positions 1 and 3 (2 and 4) is small, the condition (15) can be met in DyCrO_3 if $a_0 \neq 0$.

The presence of the d -subsystem can thus alter qualitatively the character of the metamagnetic transition in a rare-earth subsystem by renormalizing the R-R interaction constants via isotropic R-Cr exchange. An important role is played in this case by the orientation of the Ising axis; it must be closer to the b axis of the crystal ($\cos 2\alpha < 0$). This shows also that the physical cause of the two-step metamagnetic transition is the energy gained (at $\cos 2\alpha < 0$) by the intermediate phase D through the additional tilt of the magnetic moments of the Cr subsystem towards the b axis when a nonzero magnetization of the Dy^{3+} ions appears in this direction. The size of this tilt in phase D is

$$F_y = 1/2 \mu_0 a_0 \sin \alpha / 2H_E \mu_{Cr}. \quad (16)$$

For $a_0 = -(1-1.5) \cdot 10^5$ Oe (Ref. 16), $\mu_0 = 9.4 \mu_B$, $\alpha = 63^\circ$, $\mu_{Cr} = 3 \mu_B$, and $H_E \approx 2 \cdot 10^6$ Oe we get $F_y \approx -(3-5) \cdot 10^{-2}$.

The fields of the metamagnetic transitions $A \leftrightarrow D$ and $D \rightarrow B$ are accordingly

$$H_{x1,2} = H_{x0} \mp \Delta H,$$

where

$$H_{x0} = h_{x0} / \mu_0 \cos \alpha - H_{\text{eff}}^x, \quad \Delta H = -\tilde{T}_{13} / \mu_0 \cos \alpha.$$

Let us estimate the difference $H_{x2} - H_{x1} = 2\Delta H$ between the transition fields. Neglecting T_{13} in (15) we get for the parameter given above $H_{x2} - H_{x1} \approx 10$ kOe, in agreement with our experimental data and with the results of Refs. 7 and 8.

We now analyze the character of the spontaneous transition into an antiferromagnetically-ordered state of the Dy subsystem. A feature of this transition is that it takes place in an internal effective field acting on the Dy^{3+} ions and applied by the Cr subsystem along the a axis. From this standpoint, this transition is analogous to a transition into an antiferromagnetic state in a usual metamagnet in an external magnetic field. Obviously, this field lowers the magnetic-ordering temperature T_{N2} . Two situations are possible then. If the external (or effective internal) field is weaker than the field corresponding to the tricritical point, the ordering proceeds smoothly, via a second-order phase transition. In the opposite case the ordering should occur discontinuously,

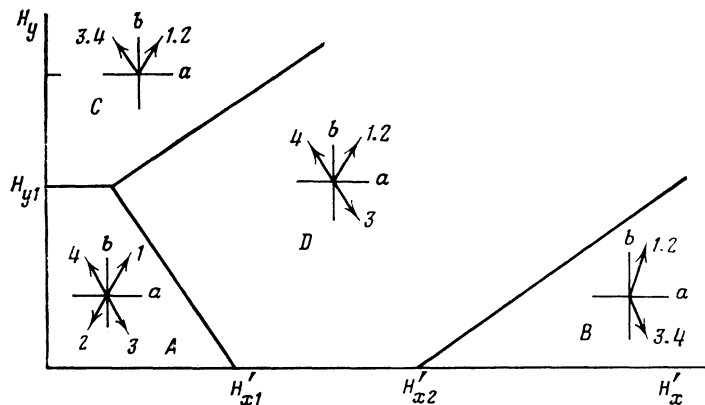


FIG. 6. $H'_x - H_y$ ($H'_x = H_x + H_{\text{eff}}^x$) phase diagram for DyCrO_3 at $T = 0$ K. Phase A corresponds to the configuration $(g_x a_y)$, B to $(f_x c_y)$, C to $(f_y c_x)$, and D to $(g_{xy} a_{yx} f_{xy})$.

i.e., via a first-order phase transition. It is important to note here that if the sample has finite dimensions, an intermediate state,^{17,18} in which domains of the phases Γ_2 and Γ_{25} coexist, sets in near such a phase transition. The transition thus extends over a certain temperature interval in which the susceptibility of the system should be constant. It is possible that a similar situation was observed in our experiments on DyCrO_3 (see Fig. 2). The quantitative estimates of the susceptibility χ_x in the phase-transition region, however, do not accord with the demagnetizing factor N_x of the sample; this seems to point to a significant role of the crystal inhomogeneities and defects, which smear out the spontaneous $\Gamma_2 \rightarrow \Gamma_{25}$ phase transition. This smearing is also manifest in the temperature dependence of the magnetization $m_x(T)$ at $T < 4$ K (inset in Fig. 2). Note that an even more smeared-out $m_x(T)$ dependence was observed in Ref. 7 (Fig. 2), apparently as a result of many imperfections of the samples used.

CONCLUSION

Let us summarize our results. Measurements and analysis of the magnetization curves for $\mathbf{H} \parallel \mathbf{a}, \mathbf{b}, \mathbf{c}$ have shown that the Dy^{3+} in DyCrO_3 behaves as an Ising ion. The effective field ($H_{\text{eff}}^x = 3.5$ kOe) that splits the ground doublet of the Dy^{3+} ion in the Γ_2 phase was determined. An $H_z - T$ phase diagram that demonstrates the presence in the ac plane of a high anisotropy energy that stabilized the Γ_2 phase was obtained. This anisotropy energy was shown not only to be related to the splitting of the ground doublet, but also to be determined to a considerable degree by the Van Vleck contribution of the Dy^{3+} ions and to the splitting of their excited doublets. A consistent analysis of the metamagnetic transitions in DyCrO_3 was carried out, with allowance of the renormalization of the Dy–Dy interaction constants by the isotropic Dy–Cr exchange. The mechanism of the two-step metamagnetic transition at $\mathbf{H} \parallel \mathbf{a}$ was shown to be connected

with the special character of the renormalization of the Dy–Dy interaction constants, governed by the circumstance that the Dy^{3+} -ion Ising axis is closer to the b axis of the crystal.

¹The quantities f, c, g and a characterize the ordering of the R subsystem with respect to the representations $\Gamma_2 (f_x c_y)$, $\Gamma_3 (f_y c_x)$, $\Gamma_5 (g_x a_y)$, and $\Gamma_8 (g_y a_x)$, respectively.

¹S. Geller and E. A. Wood, *Acta Cryst.* **9**, 563 (1956).

²M. Marezio, J. P. Remeika, and P. D. Dernier, *ibid.* **B26**, 2008 (1970).

³G. Gorodetsky, B. Sharon, and S. Shtrikman, *J. Appl. Phys.* **39**, 1371 (1968).

⁴K. P. Belov, A. K. Zvezdin, A. M. Kadomtseva, and I. B. Krynetskii, *Zh. Eksp. Teor. Fiz.* **67**, 1974 (1974) [*Sov. Phys. JETP* **40**, 980 (1975)].

⁵K. P. Belov, A. K. Zvezdin, A. M. Kadomtseva, and R. Z. Levitin, *Oriental Transitions in Rare Earth Magnets* [in Russian], Nauka, 1979.

⁶T. Yamaguchi and K. Tsushing, *Phys. Rev.* **B8**, 5187 (1973).

⁷K. Tsushima, T. Tamaki, and R. Yamaura, *Proceedings, Internat. Conf. MKM-73 on Magnetism*, Nauka, 1974, Vol. V, p. 270.

⁸T. Yamaguchi, *J. Phys. Soc. Jpn.* **38**, 1270 (1975).

⁹H. Schuchert, S. Hufner, and R. Faulhaber, *Zs. Phys.* **220**, 273 (1969).

¹⁰H. Schuchert, S. Hufner, and R. Faulhaber, *ibid.* **222** 105 (1969).

¹¹L. M. Holmes, L. G. Van Uitert, R. R. Hecker, and G. W. Hull, *Phys. Rev.* **B5**, 138 (1972).

¹²A. K. Zvezdin, V. M. Matveev, A. A. Mukhin, and A. I. Popov, *Rare Earth Ions in Magnetically Ordered Crystals* [in Russian], Nauka, 1985.

¹³J. S. Jacobs, H. F. Burne, and L. M. Levenson, *Appl. Phys.* **42**, 1631 (1971).

¹⁴H. Suhl, *J. Phys. Radium* **20**, 333 (1958). T. Nakamura, *Progr. Theor. Phys.* **20**, 542 (1958).

¹⁵E. I. Golovenchits and V. A. Sanina, *Fiz. Tverd. Tela (Leningrad)* **26**, 1640 (1984) [*Sov. Phys. Solid State* **26**, 996 (1984)].

¹⁶D. V. Belov, N. P. Kolmakova, I. B. Krynetskii, *et al.*, *Zh. Eksp. Teor. Fiz.* **89**, 1063 (1985) [*Sov. Phys. JETP* **58**, 624 (1985)].

¹⁷V. G. Bar'yakhtar, A. E. Borovik, and V. A. Popov, *Pis'ma Zh. Eksp. Teor. Fiz.* **9**, 634 (1969) [*JETP Lett.* **9**, 391 (1969)]; *Zh. Eksp. Teor. Fiz.* **62**, 2233 (1972) [*Sov. Phys. JETP* **35**, 1169 (1972)].

¹⁸E. Stryjewski and N. Giordano, *Adv. Phys.* **16**, 487 (1977).

Translated by J. G. Adashko